

Carl Schmitt\*, W. P. Arnott, and J. Hallett  
Desert Research Institute, Reno NV

## 1. INTRODUCTION

Understanding the radiative properties of clouds is important to obtain a more complete understanding of earth's radiation budget. While adequate theoretical models exist for the single scattering properties of ice crystals at solar wavelengths, thermal infrared properties are difficult to obtain because exact solutions of Maxwell's equations are often needed. Laboratory measurements of ice cloud radiative properties are useful for improving the understanding of thermal infrared transfer, and for evaluation of newly developed numerical methods (Yang, et. al., 1997).

## 2. EXPERIMENTAL SETUP

A diagram of the experimental setup is shown in figure 1. The growth chamber and cloud chambers were both cooled to  $-20^{\circ}\text{C}$ . An ultrasonic nebulizer was positioned to deliver water drops into the top of the growth chamber. A cloud seeder was placed two meters from the top of the growth chamber. The seeder consisted of a looped spring that was passed through liquid nitrogen, then into the chamber. The cloud chamber was a 1m x 1m x 1.2m interior diameter freezer.

The cloud chamber had a small hole (7.5 cm diameter) in one side for the FTIR to look into, and a large hole (24 cm diameter) on the opposite side. The large hole was covered by a liquid nitrogen cooled conical blackbody. This provided a very low emission background for the experiment. A modified Bomem MB-100 spectrometer was used. Emission measurement calibration was done with software based on Revercomb (1988). Two blackbody cones of known temperature were placed by the FTIR. An uncoated flat gold mirror was used to change the FTIR's field of view from either of the calibration

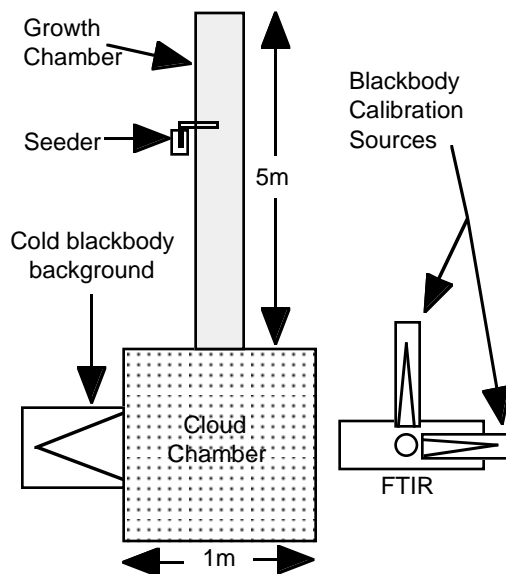


Figure 1. Side view of experimental chamber and FTIR arrangement.

blackbodies to the experimental chamber.

## 3. PARTICLE OBSERVATION

A new version of a cloudscope described in Arnott (1995) was developed and used to sample the ice crystals. A microscope objective and a compact video camera were used to image crystals. The collection surface was an optical bar of sapphire heated at the sides with a nichrome wire to sublimate ice crystals. The collection surface of the new cloudscope is 1 mm wide, and the incoming air velocity is 3 m/s. The collection efficiency of the cloudscope was estimated using principles from Langmuir (1961) and is shown in figure 2. These collection efficiencies were used only as a guideline for theoretical interpretation.

The temperature of the growth chamber was adjusted to grow different habits of ice crystals (columns and plates).

\*Corresponding author address: Carl Schmitt, Desert Research Institute, PO Box 60220, Reno, NV 89506

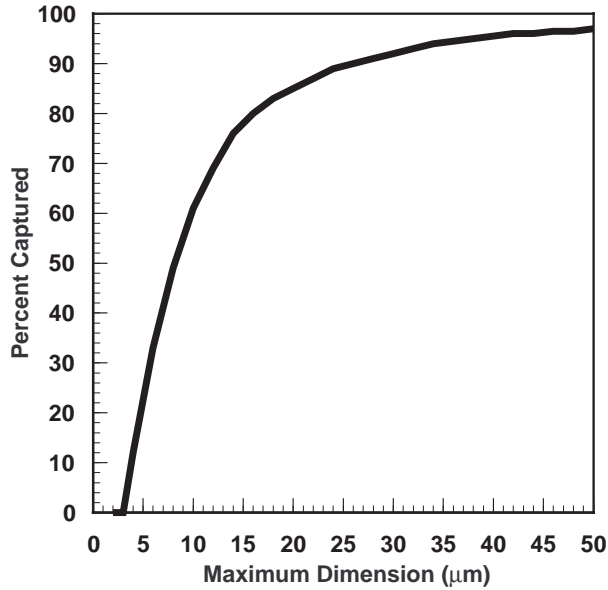


Figure 2: Cloud-scope collection efficiency.

#### 4. RESULTS

Figure 3 shows the infrared emission of the chamber with no cloud present. The large feature at  $600\text{--}700\text{ cm}^{-1}$  is caused by carbon dioxide. The spikes between  $1350\text{ and }1750\text{ cm}^{-1}$  are due to water vapor emission, as are the spikes near  $500\text{ cm}^{-1}$ . These features are visible on all lab cloud emission spectra. The  $800\text{--}1200\text{ cm}^{-1}$  atmospheric window is clearly visible. The slight rise near  $800\text{ cm}^{-1}$  is caused by a small amount of

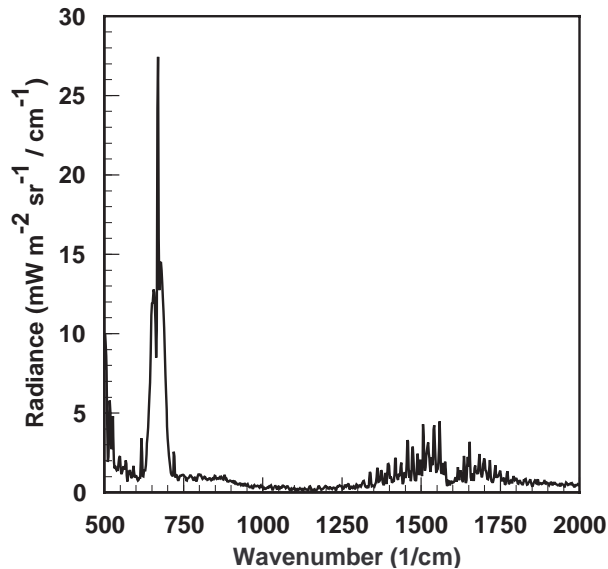


Figure 3: Cloud chamber emission with no cloud present.

cloud that forms near the cold blackbody background.

The emission from an ice cloud with a visible optical depth of 0.26 and a temperature of  $-15^\circ\text{C}$  is shown in figure 4. Carbon dioxide and water vapor emission are clearly present. The underlying smooth curve is due to the ice crystal cloud. The hump that extends from  $500\text{ cm}^{-1}$  to  $900\text{ cm}^{-1}$  is the main wavenumber range that shows differences with different cloud particles.

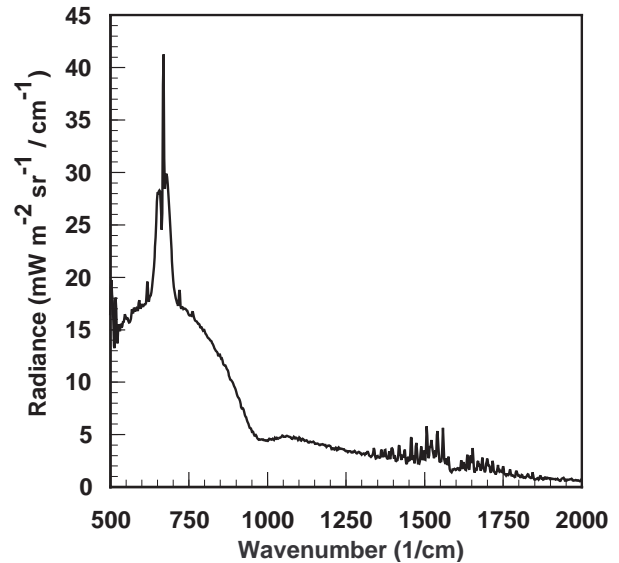


Figure 4: Emission from a lab cloud with an optical depth of 0.26 and a temperature of  $-15^\circ\text{C}$ .

The size distribution of the particles captured by the cloudscope at the same time as the measurement was being taken is shown in figure 5. The raw and collection efficiency corrected distributions are shown on the same plot.

We saw large differences in the emission spectra of the lab clouds with different crystal size distributions. The two emission spectra in figure 6 have very different shapes. The spectra were taken during times of similar visible optical depth (0.4) and temperatures ( $-9^\circ\text{C}$ ). The particles that made up the clouds were quite different though. The large bump centered near  $700\text{ cm}^{-1}$  is shifted towards higher wavenumbers for the thin lined emission spectrum.

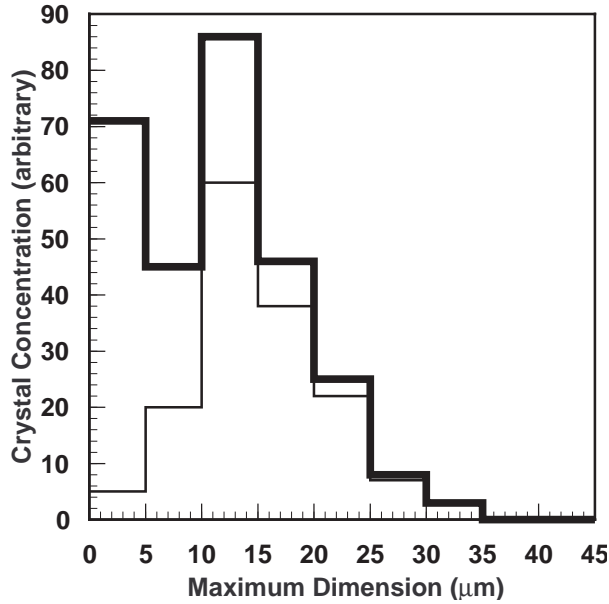


Figure 5: Size distribution of particles for measurement shown in fig 5. Bold line is adjusted by fig 2 collection efficiency. Light line is the raw data.

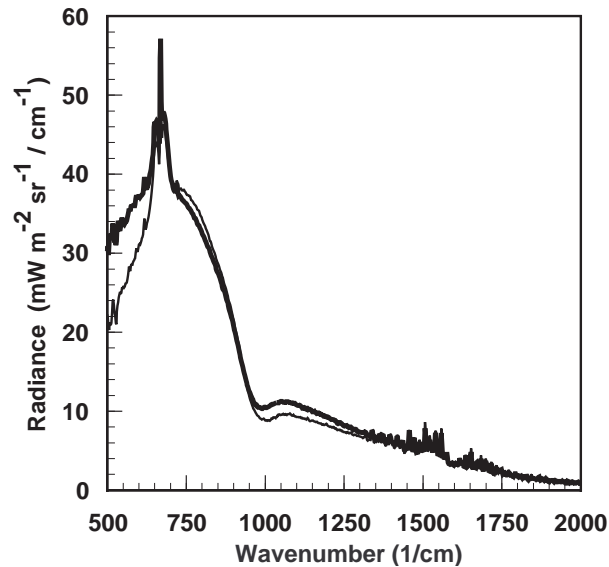


Figure 6: Two lab cloud emission spectra. The thick line is for a cloud with larger particles than the thin line spectra.

The cloudscape data for the spectra shown in figure 6 showed a high concentration of smaller particles as seen in figure 7. The crystal numbers in figure 7 are scaled by the conversion factors shown in figure 2. This was consistent with all of our results. The clouds with large numbers of

small particles usually had the hump moved towards higher wavenumbers. Larger crystal clouds showed more emission in the 500-700  $\text{cm}^{-1}$  region.

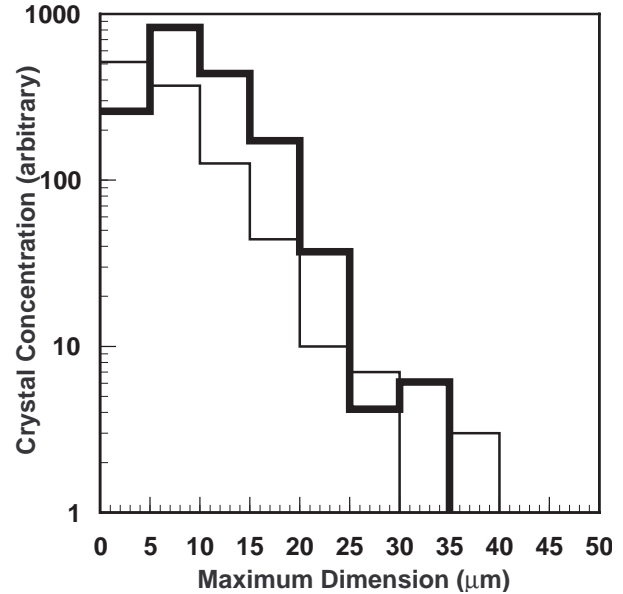


Figure 7: Collection efficiency corrected size distributions for the emission in figure 6.

*Acknowledgements:* This work was supported by NSF under grant ATM9413437.

## 5. REFERENCES

Arnott W. P., Y. Y. Dong, and J. Hallett, 1995: Extinction efficiency in the infrared (2-18 $\mu\text{m}$ ) of laboratory ice clouds: observations of scattering minima in the Christiansen bands of ice. *Appl. Opt.* **34**, 541-551.

Yang, P., K. N. Liou, and W. P. Arnott, 1997: Extinction efficiency and single scattering albedo for laboratory and natural cirrus clouds. *J. Geophys. Res.* **102**, 21,825-21,835.

Langmuir I., 1961: The collected Works of Irving Langmuir Vol 10 Atmospheric Phenomena, Pergamom Press, pp. 354-372.

Revercomb H. E., et. al., 1988: Radiometric calibration of IR Fourier transform spectrometers: solution to a problem with the High-Resolution Interferometer Sounder. *Appl. Opt.* **27**, 3210-3218.